Electronic Supplementary Information for

Methanol-assisted energy-efficient water splitting over rambutan-like Au@PdRu core-shell nanocatalysts

Hongjing Wang, Lin Cui, Shuli Yin, Hongjie Yu, Kai Deng, You Xu, Xin Wang,

Ziqiang Wang* and Liang Wang*

State Key Laboratory Breeding Base of Green-Chemical Synthesis Technology, College of Chemical Engineering, Zhejiang University of Technology, Hangzhou 310014, P. R. China.

Corresponding authors

*E-mails: zqwang@zjut.edu.cn; wangliang@zjut.edu.cn

Experimental Section

Materials Characterization

Scanning electron microscope (SEM, ZEISS Gemini 500) and transmission electron microscope (TEM, Hitachi HT 7700) were used to examine morphology and structure of samples. High-resolution TEM (HRTEM) and high angle annular dark-field scanning transmission electron microscopy (HAADF-STEM) were managed on JEOL-2100F. The crystal structure and surface state of samples were investigated by X-ray diffractometer (XRD, PANalytical X'Pert) and X-ray photoelectron spectroscopy (XPS, ESCALAB MK II spectrometer), respectively.

Electrochemical investigation

Electrochemical measurements were performed by CHI 760E electrochemical workstation in a three-electrode cell. MOR measurements were carried out in 1 M KOH + 1 M CH_3OH using Ag/AgCl electrode (KCl saturated) and Pt wire as reference electrode and counter electrode, respectively. HER measurements employed a graphite rod as a counter electrode and Hg/HgO electrode as a reference electrode in 1 M KOH. To obtain working electrode, catalyst ink was prepared by adding 5 mg of catalyst in 0.6 mL of water, 0.3 mL of ethanol and 0.1 mL of Nafion (0.5 wt%), and then 2 μL of catalyst ink was dropped onto a polished glassy carbon electrode (GCE) for drying at 50 °C. Linear sweep voltammetry (LSV) is carried out at the scan rate of 5 mV s^{-1}. Prior to each electrochemical test, the solutions were purged with nitrogen for 30 min. All the HER polarization curves were based on *iR* correction using the equation: $E_{corrected} = E_{measured} - iR$, where *i* is the current and *R* is the uncompensated electrolyte ohmic resistance measured by electrochemical impedance spectroscopy (EIS), respectively. Tafel slope was acquired from fitted LSV curves according to the Tafel equation ($\eta = a \times \log(j) + b$, where η is overpotential, a is Tafel slope, and *j* is

current density). Chronopotentiometry (*V–t*) was conducted to estimate catalyst durability. EIS was carried out in the range of 100 mHz to 100 kHz at 0.82 and -0.2 V for MOR and HER, respectively. Electrochemical active surface area (ECSA) was calculated from cyclic voltammograms (CVs) based on the equation (ECSA = $Q/(m\times420)$, where m is Pd mass loading, 420 μC cm^{-2} is reduction charge of Pd oxide monolayer on the Pd surface, and Q is acquired by integrating the reduction charge of the Pd oxide layer). Catalyst inks were doped on carbon paper (CP) with a mass loading of 0.5 mg cm^{-2} for the two-electrode HER-MOR system.

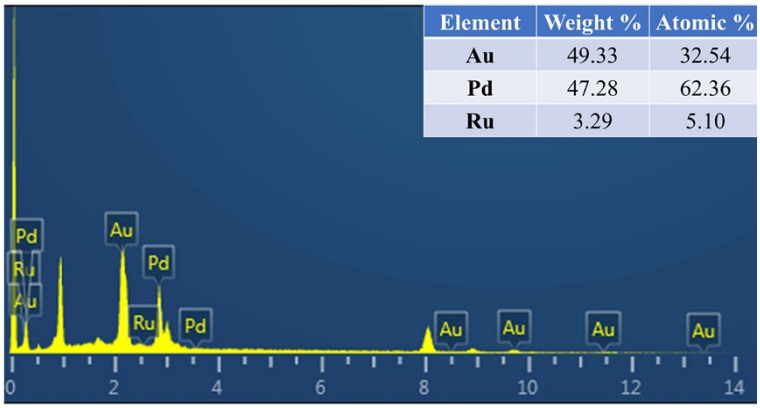

Element	Weight %	Atomic %
Au	49.33	32.54
Pd	47.28	62.36
Ru	3.29	5.10

Fig. S1 EDX spectrum of the Au@PdRu RNs.

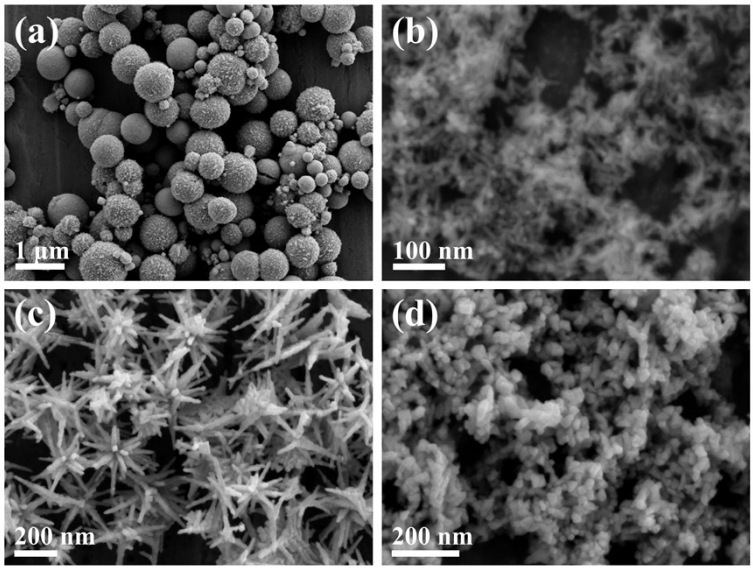

Fig. S2 SEM images of the prepared samples with different dosages of KBr under the typical synthesis conditions: (a) 0 mg, (b) 40 mg (c) 80 mg and (d) 160 mg.

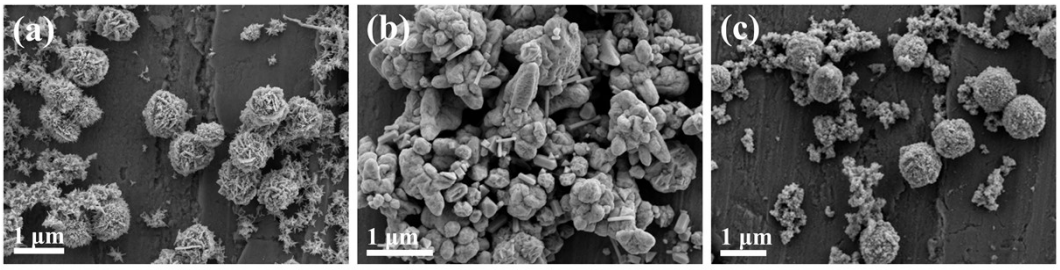

Fig. S3 SEM images of the prepared samples with different dosages of surfactant under the typical synthesis conditions: (a) F127, (b) CTAC and (c) PVP.

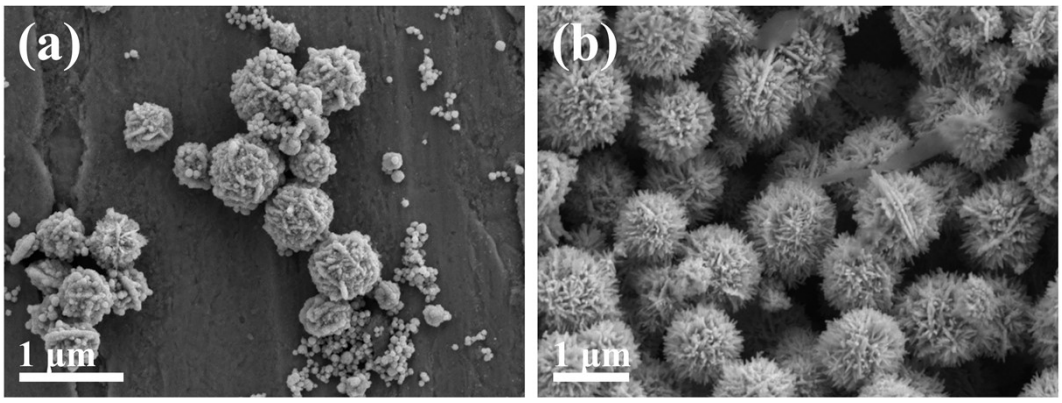

Fig. S4 SEM images of the prepared samples with different dosages of HCl under the typical synthesis conditions: (a) 0 mL and (b) 0.1 mL.

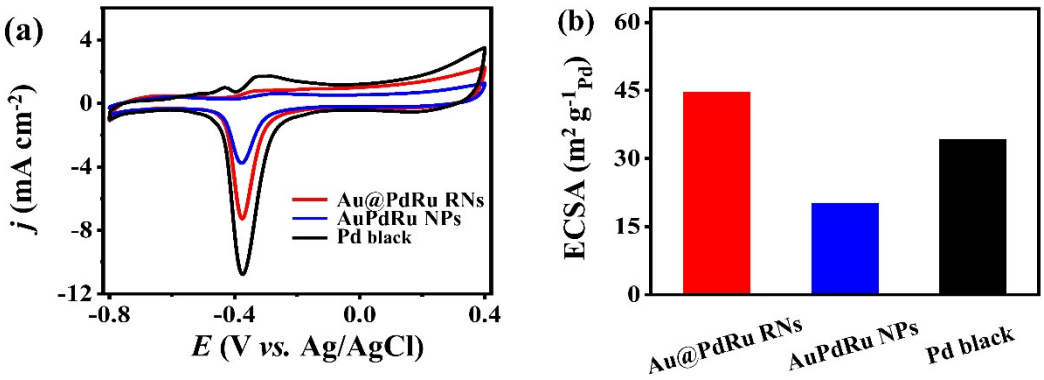

Fig. S5 (a) CV curves of the different catalysts in 1 M KOH solution at a scan rate of 50 mV s^{-1} and (b) corresponding ECSA of different catalysts.

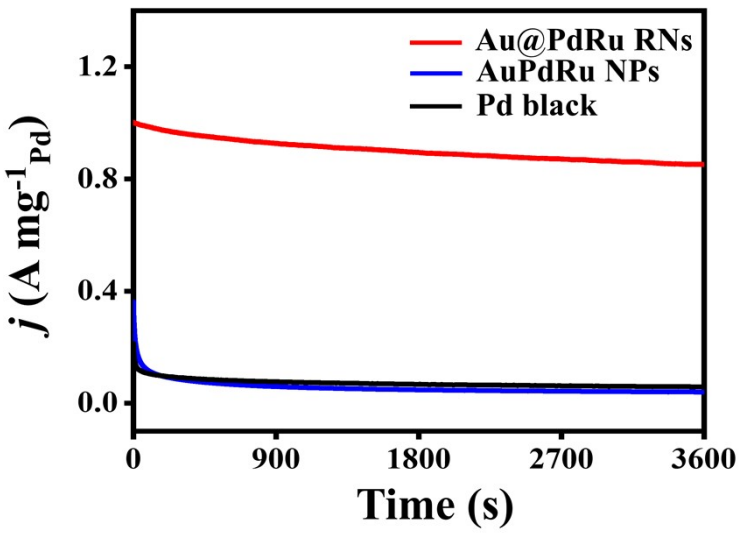

Fig. S6 Chronoamperometric curves of samples at −0.25 V.

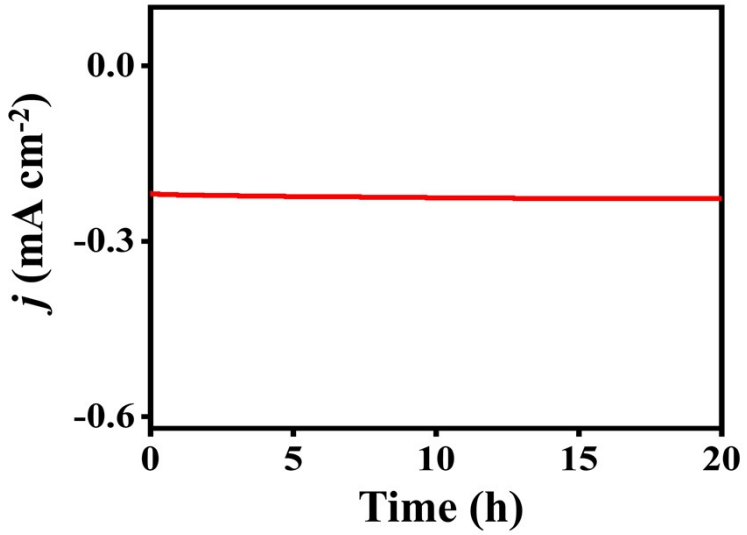

Fig. S7 Chronopotentiometry curve for the Au@PdRu RNs at a constant cathodic current density of 10 mA cm^{-2} in 1 M KOH electrolyte for 20 h.

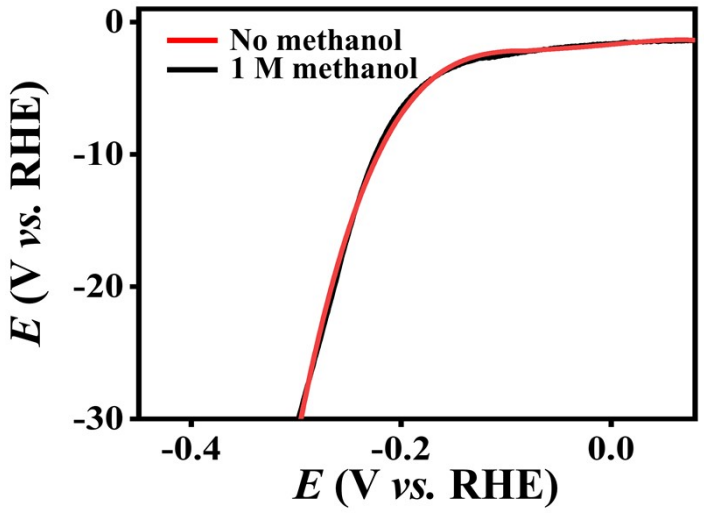

Fig. S8 HER polarization curves for the Au@PdRu RNs in 1 M KOH electrolyte without and with 1 M CH_3OH.

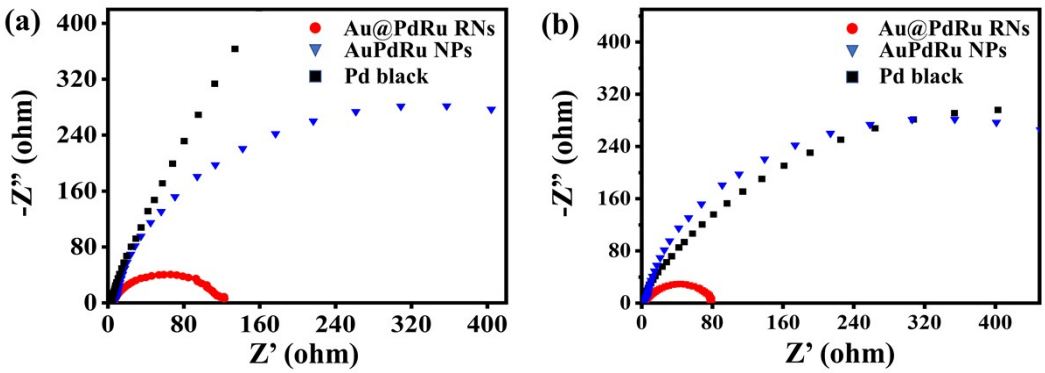

Fig. S9 EIS spectra of various electrocatalysts in 1 M KOH with and without 1 M CH_3OH under different applied potentials of (a) 0.82 V (vs. RHE) and (b) -0.2 V (vs. RHE), respectively.

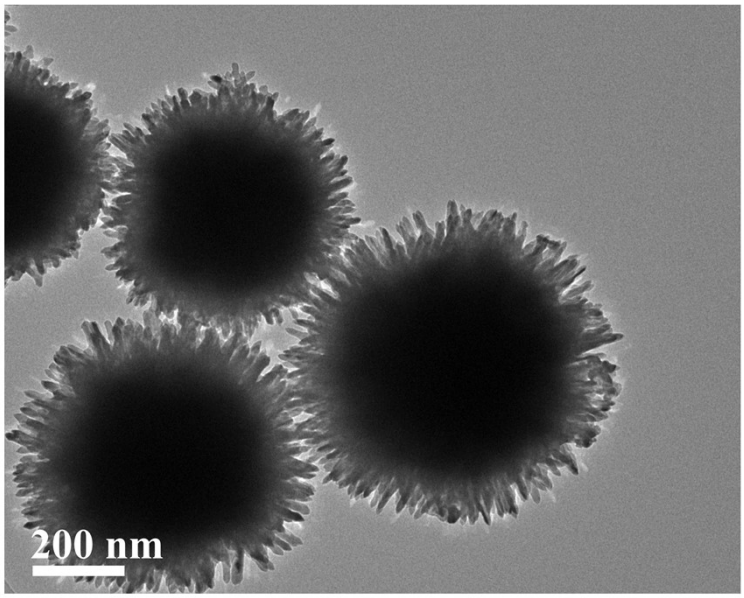

Fig. S10 TEM image of the Au@PdRu RNs after catalytic stability test.

Table S1. The mass activity of Au@PdRu RNs compared with several recently reported MOR electrocatalysts.

Catalyst	Condition	Scan rate ($mV\ s^{-1}$)	Mass activity ($A\ mg^{-1}_{Pd}$)	Ref.
Au@PdRu RNs	**1 M KOH + 1 M CH_3OH**	**50**	**1.56**	**This work**
Bowl-like PdCu	1 M KOH + 1 M CH_3OH	50	1.46	1
PdCuCo/rGO	1 M KOH + 1 M CH_3OH	50	1.06	2
Pd_1Cu_5	1 M KOH + 1 M CH_3OH	50	1.09	3
PdCu/VrGO	1 M KOH + 1 M CH_3OH	50	0.76	4
Pd_2P_1	1 M KOH + 1 M CH_3OH	50	0.87	5
Pd-PdO PNTs	1 M KOH + 1 M CH_3OH	50	1.11	6
Pd-CeO_2/SCS	1 M KOH + 1 M CH_3OH	50	0.90	7
Pd−Co J-NWs	1 M KOH + 1 M CH_3OH	50	1.21	8

Table S2. The cell voltage of Au@PdRu RNs||Au@PdRu RNs methanol electrolyzer compared with several small molecule oxidation assisted water electrolysis.

Catalyst	Substrate molecule	Cell voltage (V)	Stability (h)	Ref.
Au@PdRu RNs	**methanol**	**0.88**	**20**	**This work**
NC/Ni-Mo-N/NF	glycerol	1.38	12	9
Ni_2P nanomeshes	benzylamine	1.41	40	10
$Co(OH)_2$@HOS/CP	methanol	1.49	20	11
Fe_2P films	glucose	1.22	24	12
Co-Ni alloy	glucose	1.39	12	13
Pt-NP/NiO-NS	methanol	1.39	14	14

References

1. S.-Q. Liu, Y.-T. Xu, J.-Q. Xie, G.-Q. Sheng, Y.-W. Zhu, X.-Z. Fu, R. Sun and C.-P. Wong, *ACS Appl. Energy Mater.*, 2018, **1**, 3323-3330.
2. F. Yang, B. Zhang, S. Dong, C. Wang, A. Feng, X. Fan and Y. Li, *J. Energy Chem.*, 2019, **29**, 72-78.
3. J. Sheng, J. Kang, H. Ye, J. Xie, B. Zhao, X.-Z. Fu, Y. Yu, R. Sun and C.-P. Wong, *J. Mater. Chem. A*, 2018, **6**, 3906-3912.
4. L. Yang, D. Yan, C. Liu, H. Song, Y. Tang, S. Luo and M. Liu, *J. Power Sources*, 2015, **278**, 725-732.
5. K. Zhang, C. Wang, D. Bin, J. Wang, B. Yan, Y. Shiraishi and Y. Du, *Catal. Sci. Technol.*, 2016, **6**, 6441-6447.
6. T. J. Wang, F. M. Li, H. Huang, S. W. Yin, P. Chen, P. J. Jin and Y. Chen, *Adv. Funct. Mater.*, 2020, **30**, 2000534.
7. Q. Tan, C. Shu, J. Abbott, Q. Zhao, L. Liu, T. Qu, Y. Chen, H. Zhu, Y. Liu and G. Wu, *ACS Catal.*, 2019, **9**, 6362-6371.
8. C. Wang, L. Zheng, R. Chang, L. Du, C. Zhu, D. Geng and D. Yang, *ACS Appl. Mater. Interfaces*, 2018, **10**, 29965-29971.
9. Y. Xu, M. Liu, S. Wang, K. Ren, M. Wang, Z. Wang, X. Li, L. Wang and H. Wang, *Appl. Catal., B*, 2021, **298**, 120493.
10. Y. Ding, B.-Q. Miao, S.-N. Li, Y.-C. Jiang, Y.-Y. Liu, H.-C. Yao and Y. Chen, *Appl. Catal., B*, 2020, **268**, 118393.
11. K. Xiang, D. Wu, X. Deng, M. Li, S. Chen, P. Hao, X. Guo, J. L. Luo and X. Z. Fu, *Adv.*

Funct. Mater., 2020, **30**, 1909610.

12. P. Du, J. Zhang, Y. Liu and M. Huang, *Electrochem. Commun.*, 2017, **83**, 11-15.

13. C. Lin, P. Zhang, S. Wang, Q. Zhou, B. Na, H. Li, J. Tian, Y. Zhang, C. Deng, L. Meng, J. Wu, C. Liu, J. Hu and L. Zhang, *J. Alloy Compd.*, 2020, **823**, 153784.

14. G. Ma, X. Zhang, G. Zhou and X. Wang, *Chem. Eng. J.*, 2021, **411**, 128292.